

Mirela Leskovac · Vera Kovačević · Sanja Lučić  
Hugh R. Perrott · Ivan Šmit

## Composites of Poly(Acrylate) Copolymer filled with diatomaceous earth: morphology and mechanical behaviour

Received: 1 January 2002 / Accepted: 20 February 2002 / Published online: 1 August 2002  
© Springer-Verlag 2002

**Abstract** Failure mechanisms of poly(acrylate) (PA) copolymer system filled with a diatom filler have been studied. The natural diatom filler is characterised by the original skeletal structure which allows high “inner” porosity and thus matrix penetration inside the filler particles and agglomerates of various shapes in PA composite. High diatom filler crystallinity influences the matrix re-structurization by changing the intensity ratio of matrix amorphous halos indicating the increased composite film inhomogeneity. Interactions at the interface between diatom filler and PA copolymer matrix, specially for coarse cylindrical-shaped particles are low, showing low adhesion in the composite. We see composite weakening with the increased filler volume fraction, i.e. lowering the composite strength at break as a consequence of lower degree of interactions. On the other hand, the composite modulus and the yield strength increased as a result of matrix hardening due to the pronounced matrix penetration inside the porous diatom filler. The mechanisms of failure depend on the location with the lowest product of composite module and break energy. Because dewetting occurred, it is the product *EG* in the interfacial region between PA matrix and diatom filler particles that was relevant. The effects of filler characteristics, may be followed through an interaction coefficients calculated from a model equations. The numerical values of coefficients in the model are only comparative, but the relative values can be connected with changes at the interface.

**Keywords** Diatomaceous earth-Morphology · Mechanical behaviour · Poly(acrylate) composite

### Introduction

Scanning electron microscopy (SEM) is widely applied to investigate the interfacial adhesion in filled composites, generally through examination of fracture surfaces [1]. This technique is specially useful for the observation of the surface structure of film samples, while the thin transparent films can be examined directly by SEM [2]. We have prepared the poly(acrylate) (PA) composite samples in the form of thin films and examined them before and after the film fracture.

The main interest was related on the effect of diatomaceous earth as a filler on the deformation mechanisms and mechanical properties of composites based on the PA copolymer matrix. Diatomaceous comes from the word diatom, which is the single celled aquatic plant. Diatoms are living phytoplanktons which form an important part of marine and freshwater. The silicate shell, termed “frustule” supports a fleshy body [3]. The fossil beds are skeletons sunk to the bed of lake or sea after as the body died and formed deposits there. Diatoms are found in a great variety of forms [3]. The skeletal remains of diatoms with sub-micron-sized holes, are described as “indescribable particle shape” far from any simple classification [4].

The first use of diatom in composites was in 1864, by the founder of Nobel Prizes, Alfred Nobel, who mixed nitro-glycerine with a diatom to make dynamite. The high porosity and low density of diatom filler rendered the nitro-glycerine matrix safe to handle [3].

The specific diatom morphology and chemical resistance could be the base of using this material as a filler in composites. There is little in the literature on this subject. Adhesion between matrix and filler phases in composites is important in crack propagation and composite failure. The study of the deformation and failure process, their relation to the structure of composite and the

Vera Kovačević · Mirela Leskovac (✉) · Sanja Lučić  
Faculty of Chemical Engineering and Technology,  
University of Zagreb Marulićev trg 19, 10000 Zagreb, Croatia  
e-mail: melesko@marie.fkit.hr  
Tel.: ++385-1-4846378, Fax: ++385-1-4597260

Hugh R. Perrott  
Centre for Electron Optical Studies, University of Bath,  
BA2 7AY, UK

Ivan Šmit  
Ruder Bošković Institute, Bienička 6, 10000 Zagreb, Croatia

strength of interactions between the PA matrix and filler phases may provide useful information for the development of the new composite materials with diatoms.

## Experimental

### Materials

All samples used were commercial grade, used without further purification. The poly(acrylate) (PA) copolymer matrix, Acronal (styrene-butyl acrylate-ethylbenzene-acrylamide and formaldehyde) from BASF, Germany, were used. The filler sample of diatomaceous earth (diatom) was used. The ore is actually the skeletal remains of plankton. The natural powder was subjected to calcination after the ore milling and air-drying. The commercial sample (Celatom MW27, Solvay, Germany) used has the following characteristics; mean particle size  $13\ \mu\text{m}$  (1–48  $\mu\text{m}$  range); chemical composition (%):  $\text{SiO}_2$  (88.8),  $\text{Al}_2\text{O}_3$  (4.6),  $\text{Fe}_2\text{O}_3$  (1.5),  $\text{CaO}$  (1.2),  $\text{MgO}$  (0.2), other oxides (3.7).

### Film sample preparation

Samples were prepared by mixing (1000 s/min, 5 min) of PA commercial water dispersion ( $50 \pm 1\%$ ) with volume fractions of the diatom filler,  $\phi_f$  (%) = 3, 6, 9, 12 ( $\rho_{\text{PA}} = 1.08\ \text{g/cm}^3$ ,  $\rho_{\text{diatom}} = 2.35\ \text{g/cm}^3$ ). Film samples used for testing were prepared on polyethylene foils and dried to a constant weight (thickness 0.2 mm).

### Experimental techniques

Scanning electron microscopy (SEM) analysis of the diatom filler and PA composite films were performed with a JEOL JSM-T330.

Wide angle X-ray diffraction experiments (WAXD) were made on a Philips diffractometer with monochromatic  $\text{CuK}\alpha$  radiation in the range of Bragg's angle  $2\theta = 4\text{--}60^\circ$ .

Differential scanning calorimetry (DSC) measurements with the heating rate of  $10\ ^\circ\text{C}/\text{min}$  and a sample size of 8.5–9.5 mg, were carried out with Universal V 18 MTA instrument.

The film samples ( $50 \times 15\ \text{mm}$ ) were strained to the break by simple tensile testing using a Zwick 1445 Universal testing machine, with the crosshead speed of  $25\ \text{mm}/\text{min}$ .

## Results and discussion

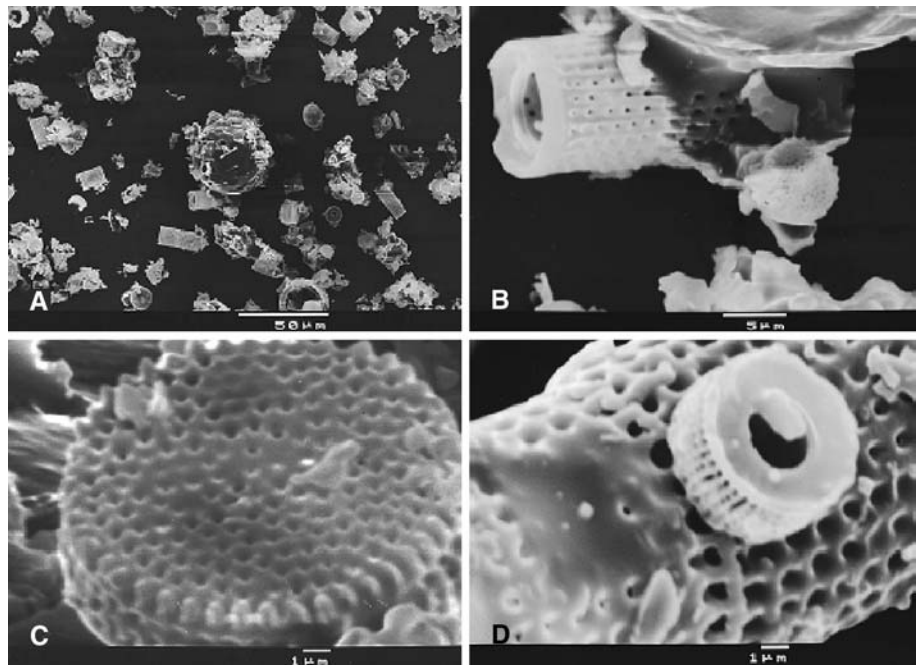
### Filler characterization

SEM micrographs of diatom filler particles show a variety of shapes. A classical illustration of “indescribable” particle shape may be seen in photomicrographs [4]. The diatom filler particles were grounded and processed before, so their fragments have an even greater variety of shapes. The characteristic circular and cylindrical-shaped particles and/or their agglomerates with characteristic sub-micron-sized holes of investigated diatom filler are visible in Figure 1.

Visible “inner” porosity of fossil diatom skeletons, is the consequence of reproduction cycles of living diatoms. Reproduction takes place generally by cell division. The new daughter valve is formed inside the parent. Thus each daughter cell is smaller than the parent, because the new valve is built within the parent valve to a point when the reduction goes no further. Then the living portion enlarges and forms two new larger valves, and the whole process re-commences [3].

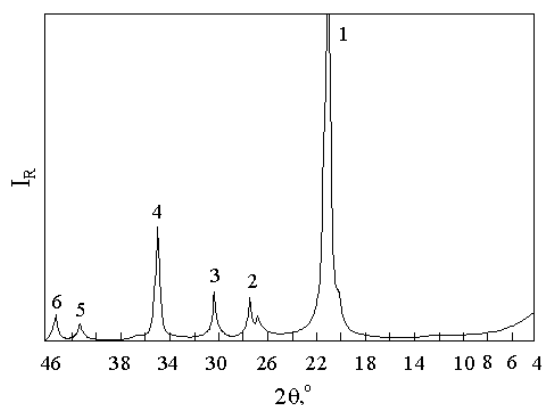
The natural diatom filler porosity is considered to be of importance in applications of diatom filler in composites, as there is the possibility of matrix penetration into the filler. The wide varieties of particle shapes, along with the agglomerates, could be expected to influence the composite film continuity and thus the mechanical properties.

**Fig. 1** SEM micrographs of diatom filler particles showing a variety of shapes (A), with characteristic cylindrical (B) and circular “stubby cheese” shape (C) and their agglomerates (D)



**Table 1** X-ray analysis of diatom filler. (Figure 2)

Nr.	Experiment Diatom		Assignment structure Opal-C [5]	
	$d/\text{\AA}$	$I/I_1$	$d/\text{\AA}$	$I/I_1$
1	4.29	9	4.08	100
	4.09	100		
	3.24	2		
2	3.16	6	3.14	9
	2.87	7		
3	2.87	7	2.86	10
	2.50	18		
4	2.50	18	2.51	30
	2.39	<1		
5	2.13	2	2.13	4
	2.04	3		
6	1.95	2	1.94	5
	1.89	2		
	1.70	1		
	1.70	1		
	1.62	4		

**Fig. 2** X-ray patterns of the diatom filler (Table 1)

The strongly bonded particles observed in Figure 1, are aggregates. The aggregation opens the possibilities of crack initiation and lower deformability of composites. The less strongly bonded agglomerates may act also as the potential points of stress concentration in the composites.

The microscopic observation of diatom fillers was complemented by X-ray diffraction, the results of which

are shown in Table 1 and Figure 2. Experimental diffraction data (interplanar spacing  $d$  and relative intensity,  $I/I_1$  for diatom filler) were compared to the corresponding literature values for opaline silica polymorphs Opal-A, Opal-C, Opal-CT ( $\text{SiO}_2 \cdot \text{H}_2\text{O}$ ),  $\alpha$ -cristoballite ( $\text{SiO}_2$ ), and  $\alpha$ -trimidite ( $\text{SiO}_2$ ) [5]. The best fitting of the experimental interplanar spacings was found for Opal-C (Table 1).

Diatomaceous earth is primarily an amorphous silica [4, 6], but in our study diffractograms of diatom filler showed a high degree of crystallinity (content of amorphous phase  $w_a \cong 9\%$ ), with the crystal phase close to the opal-C (Table 1).

### Morphology of PA composite with diatom filler

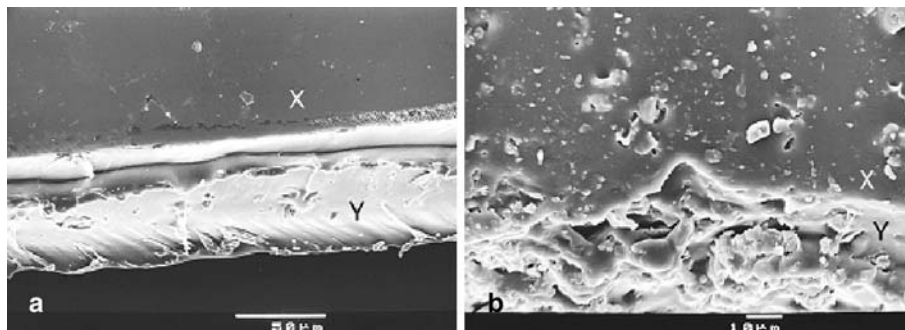
The unstrained film of PA matrix showed a flat homogeneous surface typical of an air-dried polymer film (Figure 3a). The surface of the composite film becomes un-homogeneous by the addition of diatom filler (Figure 3b). Polymer matrix partly covered the aggregate of diatom particles by penetrating more or less inside the filler.

The structure of the films at much finer level was examined by wide-angle X-ray diffraction (Figure 4)

The WAXD pattern of PA matrix exhibit two amorphous diffraction halos with intensity maxima which correspond to the Bragg's spacings,  $d_1 = 1.052$  nm and  $d_2 = 0.459$  nm (Figure 4A). The additive crystalline pattern (sharp maxima) in the composite sample belongs to diatom filler (Table 1, Figure 4B). The tops of amorphous maxima ( $d_1$  and  $d_2$ ) showed both a shift to the lower  $d$ -values caused by introducing the filler. The amorphous diffraction maximum,  $d_1 = 1.052$  nm, which corresponds to the intermolecular character of PA copolymer matrix, was shifted to  $d_1 = 0.940$  nm by filler addition. The other maximum, which corresponds to the intramolecular character of polymer matrix,  $d_2 = 0.459$  nm, showed the small shift to  $d_2 = 0.450$  nm.

The intensity ratio between the amorphous maxima for the PA copolymer matrix without filler, was changed in the composite by filler addition ( $\phi_f = 8\%$ ), from  $I_1/I_2 = 0.325$  to  $I_1/I_2 = 0.250$ . The obvious intensity decrease of the first amorphous diffraction maximum ( $I_1$ ), which is connected with interchain ( $d_1$ ) distances, to the intensity of the second maximum ( $I_2$ ), connected with intrachain

**Fig. 3** SEM micrographs of unstrained films of PA copolymer matrix (a) with homogeneous surface (x) and film edge (y) and the heterogeneous surface of the composite PA+diatom ( $\phi_f=8\%$ ) (b)



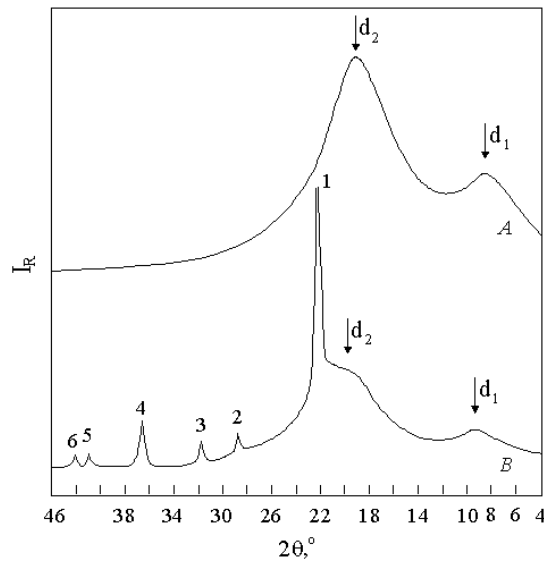
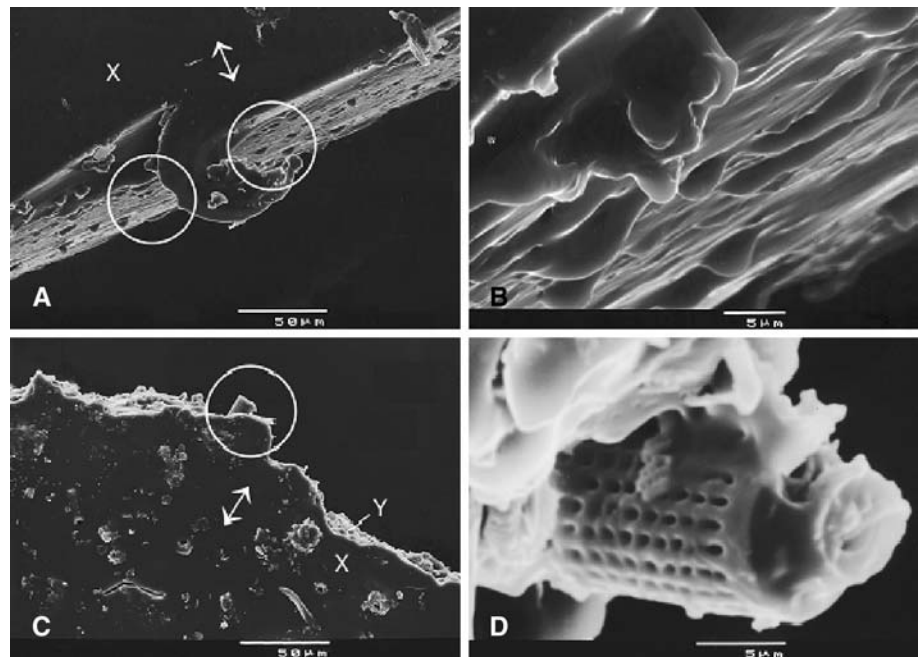


**Fig. 4** WAXD curves of films; PA copolymer matrix (A) and the composite PA+diatom ( $\phi_f=8\%$ ) (B)

distances ( $d_2$ ), when diatom filler was present, could be supposed as an indication of lowered film homogeneity. The same results were observed in our previous paper [7] for another composite system, PVAc/ $\text{CaCO}_3$  as a consequence of filler addition.

The diatom lowered the composite film homogeneity observed in SEM micrographs (Figure 3). Diatom filler addition showed the tendency of lowering the matrix interchain (intermolecular) diffraction contribution to the diffractogram of the composite sample (Figure 4), what correspond to the increased composite film inhomogeneity.

**Fig. 5** Fracture zone of films strained to break in tensile direction ( $\leftrightarrow$ ) of unfilled PA matrix (A) with a detail (B) and of the composite PA/diatom,  $\phi_f = 8\%$  (C) with a detail (D) (x = surface, y = fracture line)



The glass transition temperature of PA composite was not affected by addition of filler. The glass transition temperature for PA matrix ( $T_g = 20.4\text{ }^\circ\text{C}$ ) changed little with diatom filler addition ( $T_g = 19.5\text{ }^\circ\text{C}$ ). Similar results have been reported for PVAc composite with  $\text{CaCO}_3$  filler [7] and for polypropylene filled with  $\text{CaCO}_3$  [8]. This indicates that the filler, regardless of the degree of interactions, did not significantly affect the polymer matrix mobility in the glass transition region.

#### Failure analysis of PA composite films

Thin films were strained to break in tension. The fracture zone of strained PA matrix (Figure 5A, 5B) showed that the load was borne by PA (unfilled) amorphous matrix.

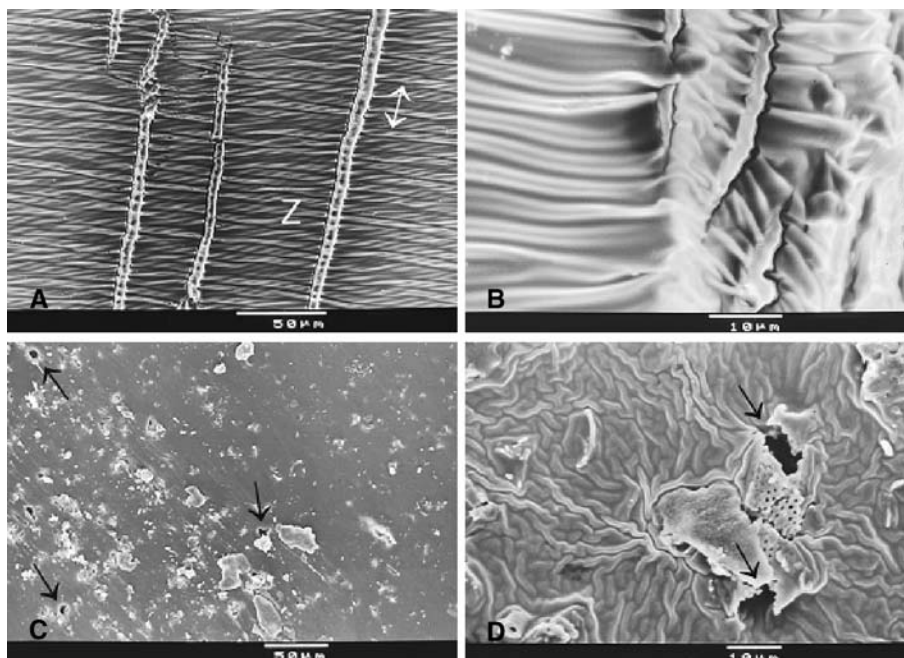
In an unfilled polymer, fracture initiates at a weakness in the structure when the local stress built up at this point. In a filled polymer failure may initiate in the matrix, or within the agglomerates of particles, or at the polymer/filler interface.

The fracture zone in the composite showed the filler particles and their aggregates partly covered by the matrix (Figure 5C). At higher magnification also visible is the matrix penetration inside the porous filler particles and separation of PA matrix from coarse cylindrical-shaped diatom particles (Figure 5D).

Failure in thermoplastics may occur by two basic deformation mechanisms: shear yielding and/or crazing. In particulate filled composites, an additional mechanism of dewetting (i.e. separation at the filler-matrix interface) can also manifest itself. These three mechanisms contribute variously to the failure in different materials.

The example of the necking area of the PA matrix, showed the fibrils perpendicular and the crazing zones

**Fig. 6** Necking area ( $z$ ) of the strained films in tensile direction ( $\leftrightarrow$ ) of PA matrix (A) with a detail (B) and of the composite (C) with visible signs of dewetting ( $\rightarrow$ ) in a detail (D)



parallel to tensile direction (Figure 6A, 6B). In the filled composite the separation between PA matrix and diatom filler at the interface by dewetting mechanisms propagated away from the defect site i.e. the coarse filler particles and/or their agglomerates (Figure 6C, 6D).

There is evidence that the mechanisms of failure in PA composite filled with diatom filler initiate at the particle edge forming cavities i.e. in a polymer layer immobilized at the particle interface by low interaction forces.

The phenomenon of dewetting was discussed in our previous paper [7]. It was concluded that the particles and/or their agglomerates above a certain size, depending on the polymer matrix and its adhesion to the filler particle, will reduce the stress needed to cause the composite to fail and fracture.

By discussing the Griffith-Irwin theory of failure in the context of adhesion, Good [9] has made a very important point that the fracture will occur when the term  $EG/r$  is the lowest, where  $EG$  is the product of modulus and the fracture energy and  $r$  is critical length of crack. Should dewetting occur, the product  $EG$  in the region adjacent to the PA matrix-diatom filler particles is relevant.

### Mechanical behaviour of PA composite filled with diatom filler

The addition of inorganic fillers to the polymer matrix affects the basic mechanical properties of the particulate-filled polymer composites. The tensile properties of the filled polymer composites are difficult to predict because they depend strongly on the local polymer-filler interactions at the interface, as well as on other factors. The interface exerts a critical effect on the properties of composites, because of its role in transferring stresses between the filler and the matrix.

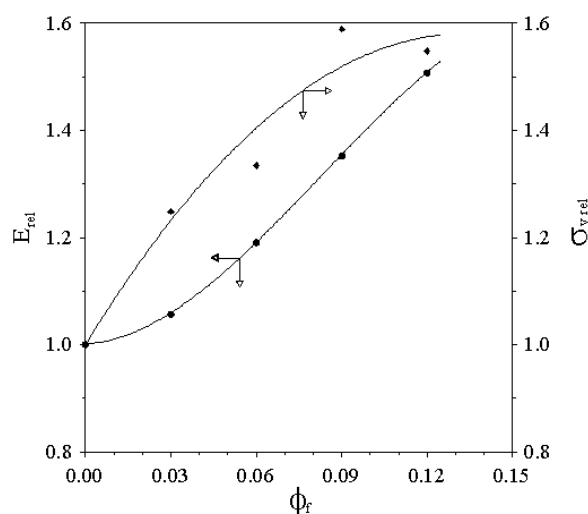


**Fig. 7** The experimental results of the relative modulus,  $E_{rel}$  (●) and the relative yield strength,  $\sigma_{yrel}$  (◆) dependence on the filler volume fraction

It is desirable to know the dependence of properties on composition (e.g. on the filler content expressed as volume fraction,  $\phi_f$ ) in order to be able to predict the optimum composition with respect to desired properties. Modification of properties in such composites depends not only on the filler volume fraction, but also on the nature of the interface between the two phases [10].

The modulus is the easiest mechanical property to predict, because it is a bulk property, which depends primarily on the shape of filler particles. The important factors are also the strength of adhesive bond between matrix and filler, the filler dispersion and the amount of particle agglomeration.

A number of equations reported in literature [11–13] relates the relative tensile modulus  $E_{rel}$  to the filler volume fraction  $\phi_f$  and describes the reinforcing action of filler particles. The experimental results in Figure 7. illustrate the reinforcing effect of diatom filler in the area of low stresses caused the expected increase in the composite modulus by filling.

However, the modulus data do not reflect the weakness in the composite structure [13] which may become apparent at higher deformations.

The relative composite yield strength measured also at lower deformations provided similar information. The results indicate, however, increased scattering of the experimental points reflecting the other factors which influenced the composite mechanical behaviour (Figure 7).

Turksanyi et al. [14] took into consideration the yield strength of the composite material  $\sigma_{yc}$  as providing information on the maximum allowable load without considerable plastic deformation:

$$\sigma_{yc} = \frac{1 - \phi_f}{1 + 2.5\phi_f} \sigma_{yp}(\phi_f) \quad (1)$$

where,  $\sigma_{yp}(\phi_f)$  which formally corresponds to the matrix yield stress is a function of the filler volume fraction.

By fitting the experimental results for many different polymer-filler systems, the change of the relative composite yield stress as a function of filler volume fraction was found to be best described by the following exponential function:

$$\sigma_{yc} = \frac{1 - \phi_f}{1 + 2.5\phi_f} \sigma_{yp} \exp(B_{yield}\phi_f) \quad (2)$$

For the various polymer+filler systems tested, it was found that they are characterized essentially by the value of parameter  $B$  for a given polymer+filler interactions [14].

The result plotted according to Equation (2) with  $B_{yield} = 4.26$  are presented in Figure 8.

On the other hand, the tensile behavior at break reflects the weakness in the composite structure which lowered the composite ultimate properties. For this reason Pukanszky [15, 16] has developed a broadened exponential model based on the ultimate tensile properties. Such characterization should give more information on the deformation and failure behaviour of the composite. The factors taken into account in Equation (3) are filler stress concentration, interfacial interactions, decrease of specimen cross section and strain hardening of the matrix:

$$\sigma_T = \sigma_{T_0} \lambda^n \frac{1 - \phi_f}{1 + 2.5\phi_f} \exp(B_{break}\phi_f) \quad (3)$$

where  $\sigma_T = \lambda\sigma$ , i.e. the true stress,  $\sigma_T$  is expressed as a function of relative elongation,  $\lambda = L/L_0$  (the actual and original length of specimen) and the engineering stress ( $\sigma$ ), respectively;  $n$  is a parameter characterizing the polymer strain hardening tendency,  $\sigma_T = \lambda^n$ . The parameter  $n$  for PA matrix was calculated from the slope of equation,

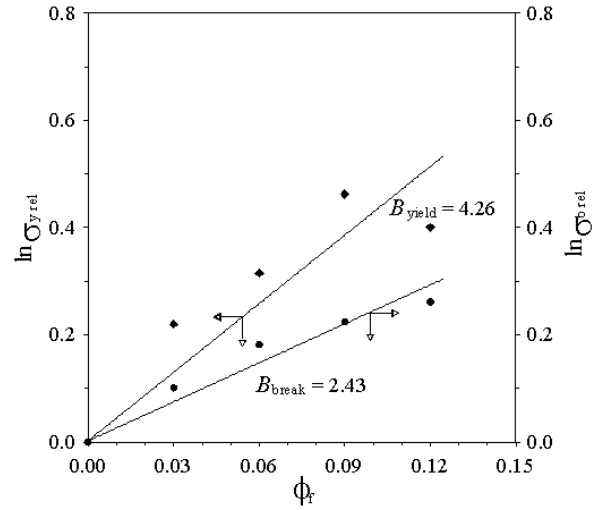


**Fig. 8** Fitting of the experimental results with Equation (2) (◆) and Equation (5) (●)

In  $\sigma_T = n \ln \lambda$  ( $n = 2.052$ ). The tensile strength increases depending on the interfacial area and on the strength of the interaction;  $\sigma_{T_{red}} = \sigma_T \exp(B\phi_f)$  ( $\sigma_{T_{red}}$  is the reduced true tensile strength,  $\sigma_{T_0}$  is the true tensile strength of polymer matrix and  $B$  is a parameter which reflects the effect of the interactions for a given polymer+filler system).

In this way in Equation (3) seems to take into account the most important factors influencing the tensile strength.

To prove the validity of Equation (3) the experimental data were evaluated according the rearranged Equations (4) and (5):

$$\sigma_{T_{red}} = \frac{\sigma_T}{\lambda^n} \frac{1 + 2.5\phi_f}{1 - \phi_f} = \sigma_{T_0} \exp(B\phi_f) \quad (4)$$

and

$$\sigma_{T_{rel}} = \frac{\sigma_{T_{red}}}{\sigma_{T_0}} = \exp(B_{break}\phi_f) \quad (5)$$

According to Equation (5), the  $\ln \sigma_{T_{rel}}$  vs.  $\phi_f$  plot should give a straight line with zero intersection [15]; see Figure 8.

In our previous papers [17, 18] we have received the above given models and fitted to the experiments for the composite systems with polyvinyl acetate (PVAc) matrix and various fillers. We have found, that if all factors of importance were taken into account, the experimental results would be fitted better to the model of the composite mechanical behavior.

The theoretical and practical utility of the model would be significantly increased if a physical meaning could be assigned to the interaction coefficient. An advantage of the exponential model is, in comparison to the other models, that it has only one interaction coefficient. Thus, the coefficient  $B$  is regarded as summarizing all the influences of the matrix, the filler and the inter-

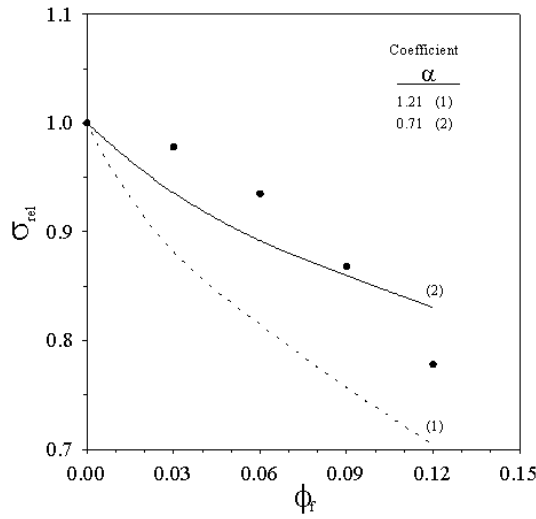


**Fig. 9** Fitting of the experimental results (●) with Equation (6) for the composite

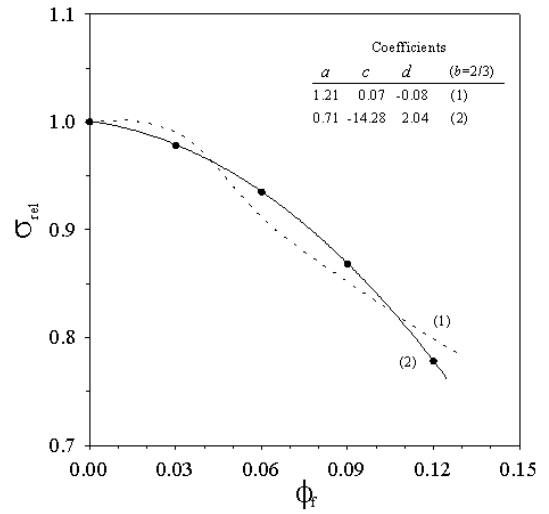


**Fig. 10** Fitting of the experimental results (●) with Equation (7) for the composite

face on the composite properties. If this is so, a conclusion about its physical meaning should be easier to draw.

The lower value of  $B_{\text{break}}$  means lower degree of interactions, in comparison to apparently higher value  $B_{\text{yield}}$  for the same composite system PA+diatom in Figure 8. This means that all factors taken into account by using Equation (5) instead of Equation (2), lowered the final true composite mechanical properties.

However, the significance of the numerical values can only be seen by comparing them with the values for other systems. For example, in our previous paper [18] the values of coefficient  $B$  for the composite system based on PVAc matrix increased accordingly with the increased degree of interactions between matrix and various fillers in order;  $\text{CaCO}_3$ , silica, and kaolin. It was interesting that in the above systems we noticed that the  $B_{\text{yield}}$  values were lower than  $B_{\text{break}}$ , opposite to the system with diatom filler in this paper.

The special effect of diatom filler, caused higher coefficient  $B_{\text{yield}}$ , possibly due to the observed pronounced matrix penetration into the filler. This could lead to the potential use of diatom fillers for composites where stresses in service remain low enough.

On the other hand, the coefficient for the PA+diatom composite at higher stresses ( $B_{\text{break}} = 2.43$ ) was much lower than for example for the composite with PVAc matrix with  $\text{CaCO}_3$  filler ( $B_{\text{break}} = 6.36$ ) or with kaolin ( $B_{\text{break}} = 18.30$ ) [18]. Although  $B$  has no direct physical meaning, it is obviously connected with the interfacial properties [14]. The examples given above illustrate that the higher value of  $B$  coefficient indicates the composite reinforcing; when  $B$  is lower, as in the present case, the composite weakening.

In the absence or for low adhesion between the polymer matrix and the filler (i.e. for the composite weakening) a different model of composite mechanical behavior [19] was also explored:

$$\sigma_{\text{rel}} = \sigma_c / \sigma_p = 1 - \alpha \phi_f^{2/3} \quad (6)$$

where the coefficient  $\alpha$  is related to the stress concentration caused by filler particles; thus the higher values mean higher stress concentration effects. The parameter  $n=2/3$  is related to the geometry of the non spherical filler, when the sample fails by random fracture.

The experimental results were fitted to the model given by Equation (6) in Figure 9.

The experimental data did not fit well either for  $\alpha=1.21$  or for  $\alpha=0.71$  (Figure 9). It is obvious that the approximate coefficient closer to the experiment should be lower than the value ( $\alpha < 1.21$ ) indicating the case of better adhesion between matrix and filler [11].

Analysing the numerical values of coefficients calculated from the appropriate model equations in Figure 9, it should be stressed again that the significance of the numerical values can only be seen by comparing them with values for other systems. For example, the  $\alpha=1.21$  fits in well with the data for SAN+aluminium composite [11], where there is practically no adhesion between aluminium particles and the matrix. Another example from literature, when  $\sigma_{\text{rel}}$  values were higher, for example for SAN+iron composite, was an indication of streng adhesion [11].

The experimental data in Figure 9 illustrated that the better fitting was obtained with  $\alpha < 1.21$ . This is an indication of a certain level of adhesion, proved by the increased modulus and composite yield strength (Figure 8), regardless the final composite weakening (Figure 9).

For the case of adhesion (i.e. for composite reinforcing) which accounts for the improved adhesion between matrix and filler, the competing loss in strength owing to stress concentration points at the polymer+filler interface should be also taken into account in the model expanded from Equation (6) on a purely empirical basis [20]:

$$\sigma_{\text{rel}} = 1 - a\phi_f^b + c\phi_f^d \quad (7)$$

where  $a$  (or  $\alpha$ ) and  $b = 2/3$  are seen in Equation (6), with different coefficients  $c$  and  $d$  calculated from the experimental data as the indicators of the strength of adhesion.

Most of the composite systems fail somewhere in-between these two boundary cases.

The best fit again (curve 2 in Figure 10) was obtained with the coefficient  $a < 1.21$  ( $a = 0.14$ ), indicating some degree of interactions at the interface between the PA matrix and diatom filler.

It should be noted that the reinforcing effect may be lost as the filler concentration increases. Many systems show a modest degree of reinforcement at low filler concentrations and loss in tensile strength at higher concentrations. The addition of filler particles gives rise to local defects that induce critical effects influencing the strength of the matrix.

Thus, the coefficients  $c$  and  $d$ , calculated from the experimental data should be indicators of the strength of adhesion to the extent that reinforcement is achieved [20]. Again the examples from literature indicated that the lower calculated values of  $c$  and  $d$  for ABS+talk than for Noryl+talk composites [20] indicate less adhesion between the polymer and the filler.

The values of the coefficients  $c$  and  $d$  in Figure (10) for the composite are very low, or even negative, indicating the composite weakening at higher filler volume concentration. The increased composite film non-homogeneity by filler addition, the stress concentration points mostly at the edge of coarse diatom particles or their agglomerates, causing a pronounced processes of dewetting contribute to the above conclusion.

Because of the significance of interaction in the deformation and failure of composites, its quantitative estimation is very important [16]. A detailed consideration of other models which describe the composite mechanical behavior will be considered in a separate paper.

## Conclusion

Interactions at the interface between diatom filler and PA copolymer matrix are low and illustrated the case of low adhesion in composite. Mechanical properties of com-

posite showed the composite weakening with the increased filler volume fraction, i.e. lowering the composite strength at break as a consequence of lower degree of interactions. On the other hand the composite modulus and the yield strength increased as a result of matrix hardening due to the pronounced matrix penetration inside the porous diatom filler.

**Acknowledgements** We are grateful for support to the Royal Society, and British Council, London, and the Ministry of Science and Technology of Croatia, for facilitating the international collaboration between the University of Zagreb and the University of Bath through the A.L.I.S. Project. Thanks are due to Dr D.E. Packham of the University of Bath, for the ideas and advices given during the experiments and preparation of the paper.

## References

1. Rothon R (1995) Particulate-Filled Polymer Composites, Longman Scientific & Technical, Harlow, England
2. Sawyer LC and Grubb DT (1996) Polymer Microscopy, Chapman & Hall, London
3. Burton AD (1992) Microscopy & Analysis 5: 5
4. Ferrigno TH (1978) In: Katz HS and Milewski JV (ed) Handbook of Fillers and Reinforcements for Plastics, Van Nostrand Reinhold Company, New York
5. Elzea JM, Olson IE and Miles WJ (1994) Anal. Chim. Acta 286: 107
6. Seymour RB (1990) New Concepts in Polymer Science: Polymeric Composites, Utrecht, The Netherlands
7. Kovačević V, Packham DE, Lučić S, Hace D and Šmit I (1999) Polymer Eng Sci. 39: 1433
8. Jancar J (1991) J Mater Sci 26: 4123
9. Good RJ (1972) J Adhesion 4: 133
10. Packham DE (1995) J Adhesion 54: 133
11. Nicodemo L and Nicolais L (1983) J Mater Sci Lett 2: 210
12. Levita G, Marchetti A and Lazzeri A (1989) Polymer Comp 10: 39
13. Maiti SN and Lopez BH (1992) J Appl Polymer Sci 44: 353
14. Turksanyi B, Pukanszky B and Tudos F (1988) J Mater Sci Lett 7: 160
15. Pukanszky B (1990) Composites 21: 255
16. Pukanszky B (1993) Makromol Chem, Makromol Symp 70/71: 213
17. Kovačević V, Lučić S and Cerovečki Ž (1997) Int J Adhesion and Adhesives 17: 239
18. Lučić S, Kovačević V and Hace D (1998) Int J Adhesion and Adhesives 18: 115
19. Danusso G and Tieghi G (1986) Polymer 27: 1385
20. Bigg DM (1987) Polym Compos 8 (2): 115